

# Numerical Simulation of the Influencing Factors of Array Jet Shock Cooling

Nianyong Zhou<sup>1\*</sup> Youxin Zou<sup>1</sup> Yingjie Zhao<sup>1</sup> Qingguo Bao<sup>1</sup> Guanghua Tang<sup>1</sup> Wenyu Lv<sup>1</sup>

<sup>1</sup> College of urban Construction, Changzhou University, Changzhou, China

**Abstract.** Array jet impingement cooling is a significant technology of enhanced heat dissipation which is fit for high heat flux flow with large area. It is gradually applied to the cooling of electronic devices. However, The researches on the nozzle array mode and the uniformity of cooling surface still have deficiencies. Therefore, the influence of heat flux, inlet temperature, jet height, array mode and diversion structure on jet impingement cooling performance and temperature distribution uniformity is analyzed by means of numerical calculation. The results show that the heat transfer coefficient of jet impingement cooling increases linearly with the increment of heat flux and inlet temperature. With the increment of the ratio of jet height to nozzle diameter ( $H/d$ ), the heat transfer coefficient increases first and then decreases, that is, there is an optimal  $H/d$ , which makes the heat transfer performance of the array jet impact cooling best. The temperature uniformity of array jet impact cooling is greatly affected by array mode. The improvement effect of nozzle array mode on temperature uniformity is ranked as sequential > staggered > shield > elliptical array. The overall temperature uniformity and heat transfer coefficient are increased by 5.88% and 7.29% compared with elliptical array. The heat transfer performance can be further improved by adding a flow channel to the in-line array layout, in which the heat transfer coefficient is increased by 6.53% and the overall temperature uniformity is increased by 1.45%.

**Key words:** Array jet; enhanced heat exchange; numerical simulation;

## 1. INTRODUCTION

As electronic components become increasingly integrated and miniaturized, the problem of insufficient cooling has become more apparent, which hinders the further development of electronic components. Related studies have shown that prolonged use of electronic components at temperatures exceeding 85 °C will significantly reduce their reliability and lifespan [1]. The heat flux density range of existing integrated chips, laser pump sources, and other devices has already reached 100-1000 W/cm<sup>2</sup>, and traditional cooling methods are no longer able to meet the cooling needs of high heat flux density electronic components [2,3]. For high heat flux density cooling technology, there are mainly microchannel cooling, spray cooling, and jet cooling. Array jet impingement cooling is a cooling technology designed for large-area electronic components, which has advantages such as strong heat transfer performance, high energy efficiency, large cooling area, and good temperature uniformity [4-6]. Extensive research has been conducted on jet impingement cooling both domestically and internationally. Matthew[7] studied a confined array of jets and found that increasing the jet hole density can enhance the heat transfer performance. Robinson[8] investigated the impact of 21, 45, and 121 jets with different spacing in the range of

$2 < H/d < 20$  on the heat transfer performance of the surface. The results showed that when  $H/d$  is between 2 and 3, the jet spacing has no significant effect on the heat transfer performance. However, when the jet spacing is in the range of  $5 < H/d < 20$ , the average heat transfer coefficient decreases with increasing spacing. Peng[9] studied the influence of different jet heights on heat transfer performance and found an optimal ratio between  $H/d$  and  $S/d$ . When  $H/d=5$  and  $S/d=7$ , the average heat transfer coefficient of the surface reaches its maximum value. Imbriale [10] investigated the factors affecting impingement heat transfer by varying jet spacing, height, and inclination angle. The results showed that the lower the jet height, the better the heat transfer performance. Kumar et al. [11] used liquid crystal thermography to study the heat transfer performance of jet impingement cooling on porous media and found that the average Nusselt number enhancement is the highest at 52.71% and 74.68% for  $Re=400$  and 700, respectively. Kuraan et al. [12] conducted a study on water jet impingement heat transfer surfaces and analyzed the heat transfer performance and flow state. The results showed that the influence of the jet hole spacing on the heat transfer performance can be neglected when the ratio of the standoff distance to the nozzle diameter is between 1 and 0.4. Jenkins[13] investigated the effect of jet diameter on the heat transfer performance of the target surface and found that the heat transfer effect increases with increasing

\*e-mail: zhounianyong@cczu.edu.cn

nozzle diameter. Jingzhou Z[14] studied the effect of different nozzle arrangements and concluded that the cooling effect of inline nozzle holes is superior to cross arrangement when  $H/d < 3$ . Xin Y[15] found that the inline arrangement has better heat transfer performance than the staggered arrangement when studying the influence of different jet arrangements on heat transfer performance, and the heat transfer coefficient of the target heat transfer surface is highest when  $H/d = 3$ . Rhee[16] studied the jet heat transfer performance using staggered hole arrangement, square hole arrangement, and hexagonal hole arrangement. The study found that under the same conditions, the staggered hole arrangement has the best heat transfer effect, but the local Nu distribution is uneven. On the other hand, the hexagonal hole arrangement has a more uniform Nu distribution due to the increased jet hole area ratio, which can solve the problem of high thermal stress on objects.

Numerical simulation techniques have also been applied in the study of jet impingement heat transfer. Fubo Z [17] used Fluent software to simulate the process of jet impingement cooling of steel plates, and the results showed that increasing turbulent intensity can enhance heat transfer performance. Zhi L [18] simulated the air jet using the RNG k- $\epsilon$  model and found that the nozzle diameter has a negligible effect on the stagnation point Nu, while the distance between the jet hole and the target surface has a significant influence on the change of heat transfer coefficient. When the distance between the jet hole and the target surface is between 3 and 5 times the nozzle diameter, the heat transfer surface shows the highest heat transfer effect. Xin H [19] used Fluent software to simulate the jet cooling of steel plates and found that the faster the jet velocity, the better the cooling effect of the steel plate. Liu Y [20] used a novel arrangement of thin film holes and jet holes in a hexagonal pattern for numerical simulation, and the injected fluid the simulation results showed a significant increase in heat transfer on the heat transfer surface.

In summary, scholars at home and abroad have conducted certain research on jet cooling, and proposed a number of array jet-enhanced heat exchange methods, such as ribbed surface structure, jet nozzle structure, etc., and achieved more abundant research results. However, the research on array jet impact cooling still needs to be improved. Array jet impact cooling for larger areas of heat dissipation not only needs to consider cooling efficiency and effect, but also needs to optimize the uniformity of cooling. At present, there are few researches on the temperature uniformity of array jet impact cooling. This article proposes different nozzle arrangement methods and the addition of guide groove structures to explore their effects on the heat exchange performance and temperature uniformity of jet impact cooling.

## 2. Methodology

### 2.1. Computational Model.

The computational model in this study is shown in Fig 1. The overall structure consists of a cover plate, a static pressure rectification chamber, a jet hole plate, an impingement heat transfer chamber, and a bottom plate. The heat source surface

size is  $110 \text{ mm} \times 80 \text{ mm}$ , and the heat generation power is  $60\text{--}240 \text{ W/cm}^2$ . There are 20 jet nozzles.

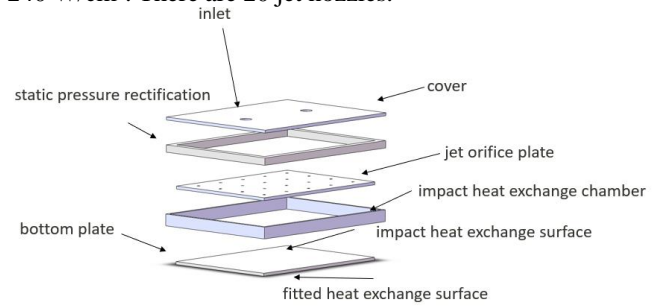


Fig. 1. Geometric Model

### 2.2. Governing Equations and Boundary Conditions.

Jet cooling is a typical two-phase flow model, so the Volume of Fluid (VOF) model is used to study the jet flow. The VOF model uses the phase fraction  $\alpha_i$  to represent the volume fraction of different phases. The volume fraction of different phases  $\alpha_i$  is given by:

$$\alpha_i = \frac{V_i}{V} \quad (1)$$

where  $V_i$  represents the volume fraction of the  $i$  phase,  $V$  represents the sum of all volume fractions.

For the incompressible fluid, the governing equation is:

$$\nabla \cdot \mathbf{u} = 0 \quad (2)$$

where  $\nabla$  is the gradient operator,  $\mathbf{u}$  is the velocity.

The continuity equation is:

$$\rho \left( \frac{\partial \mu_x}{\partial x} + \frac{\partial \mu_y}{\partial y} + \frac{\partial \mu_z}{\partial z} \right) = 0 \quad (3)$$

where  $\rho$  is the density of the injected fluid,  $\mu_x$ ,  $\mu_y$  and  $\mu_z$  are the velocity components in the three different directions, m/s.

The momentum equation is:

$$\rho \text{div}(\mathbf{u}\mathbf{u}) = -\frac{\partial p}{\partial x} + \frac{\partial \gamma_{xx}}{\partial x} + \frac{\partial \gamma_{yx}}{\partial y} + \frac{\partial \gamma_{zx}}{\partial z} \quad (4)$$

$$\rho \text{div}(\mathbf{v}\mathbf{u}) = -\frac{\partial p}{\partial y} + \frac{\partial \gamma_{xy}}{\partial x} + \frac{\partial \gamma_{yy}}{\partial y} + \frac{\partial \gamma_{zy}}{\partial z} \quad (5)$$

$$\rho \text{div}(\mathbf{w}\mathbf{u}) = -\frac{\partial p}{\partial z} + \frac{\partial \gamma_{xz}}{\partial x} + \frac{\partial \gamma_{yz}}{\partial y} + \frac{\partial \gamma_{zz}}{\partial z} \quad (6)$$

Where  $p$  represents the static pressure of the fluid, Pa;  $\gamma$  represents the dynamic viscosity,  $\text{m}^2/\text{s}$ .

The energy equation is:

$$\rho \text{div}(\mathbf{u}T) = \text{div} \left( \frac{\lambda}{c_p} \text{grad}T \right) \quad (7)$$

where  $C_p$  is the specific heat capacity in  $\text{J}/(\text{kg}\cdot\text{K})$ ,  $T$  is the thermodynamic temperature in K,  $\lambda$  is the thermal conductivity of the fluid in  $\text{W}/(\text{m}^2\cdot\text{K})$ .

In this study, water is used as the injected fluid, and the jet velocity is high. The SST k- $\Omega$  model and turbulence model are adopted for numerical simulation. The jet inlet is set as a velocity inlet, and the outlet is set as a pressure outlet. The surface which needs jet cooling is a fixed impermeable and non-slip wall, and the heat flux is  $60\text{--}240 \text{ W/cm}^2$ . The direction of the heat flow is perpendicular to the surface which needs jet cooling and it is vertically upwards. Implicit unsteady method is used for computation. The computed results can be

substituted into equation (8) to obtain the heat transfer coefficient and the non-uniformity of the temperature distribution on the impingement target surface.

$$q = h(T_w - T_f) \quad (8)$$

where  $q$  is the heat flux,  $T_w$  is the temperature on the impingement target surface,  $T_f$  is the inlet temperature of water.

$$\phi_t = \frac{\sigma_t}{\bar{t}} \quad (9)$$

$$\bar{t} = \frac{\sum t_i}{N} \quad (10)$$

$$\sigma_t = \sqrt{\frac{\sum (t_i - \bar{t})^2}{N}} \quad (11)$$

where  $\bar{t}$  represents the average temperature of all sampled points,  $t_i$  represents the temperature of the  $i$ th sampled point,  $N$  represents the number of samples,  $\sigma_t$  represents the deviation between the surface temperature and the average temperature.

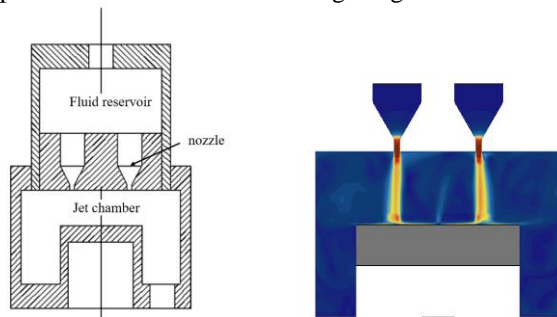
The physical properties of water are as follows:

TABLE 1. Physical Properties of Water

Temperature $t$ °C	Thermal Conductivity $\lambda$ W/(m·K)	Dynamic Viscosity $\mu$ Pa·s	Specific Heat $c_p$ J/(kg·K)	Density $\rho$ kg/m <sup>3</sup>
10	0.57871	0.001306	4195.5	999.65
20	0.59795	0.001002	4184.4	998.16
30	0.61434	0.000797	4180.1	995.61
40	0.62844	0.000653	4179.6	992.18
50	0.64057	0.000547	4181.5	988
60	0.65096	0.000466	4185.1	983.16
70	0.65972	0.000404	4190.2	977.73
80	0.66697	0.000354	4196.9	971.77
90	0.67277	0.000314	4205.3	965.3
100	0.67721	0.000282	4215.7	958.35

### 2.3. Model Validation.

In order to verify the correctness of the computational model, the experimental results of M Yu [21] are selected for comparative analysis. In the simulation, the working fluid temperature is 10°C water through a 0.8 mm diameter jet hole to impact the 20×20 mm heat exchange target surface.



(a) Design of the structure (b) Simulation structure

Fig. 2 Verify the structure and simulation structure diagram

The comparison results are shown in Fig 3. From Fig 3, it can be seen that the trend of the simulation results and the experimental results of M Yu [21] are very close under different degree of superheat. The figure 3 shows our verification of the experiment, with the minimum error of 5.5% and the maximum error of 7.1%. The biggest reason for the error is that we cannot accurately obtain the  $T_{in}$  from the paper.

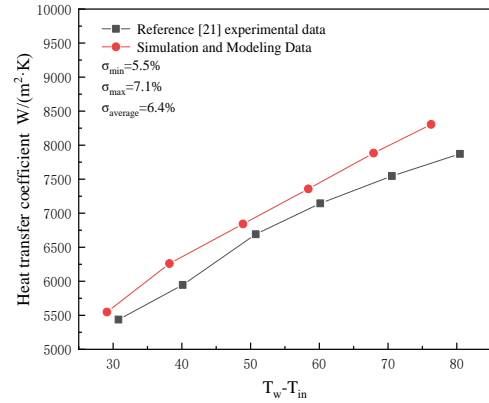
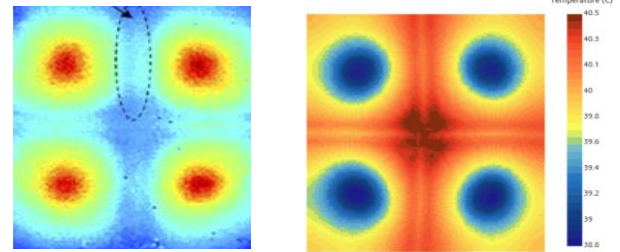


Fig. 3. Simulation and Experiment Comparison

Figure 4 (a) is the experimental result chart (From W. Wen's team [22]), and Figure 4 (b) is the cloud chart of the impact surface temperature distribution in this article at  $T_w - T_{in} = 29.2$ .



(a) experimental result [22] (b) Simulation results

Fig. 4 Comparison of Temperature Distribution Cloud Map

### 2.4. Grid independence.

The impact on simulation accuracy was verified by setting seven groups of grid numbers (Fig. 5), with the boundary parameters being a working fluid temperature of 25°C, heat flux density of 100 W/cm<sup>2</sup>, and an inlet speed of 10 m/s ( $Re = 22471$ ). The results show that when the grid number exceeds 2.84 million, the grid number has no significant impact on the simulation of this model.

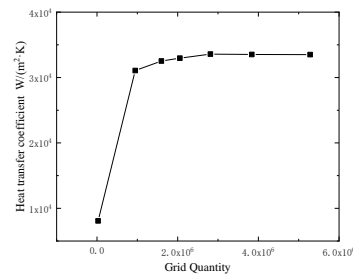
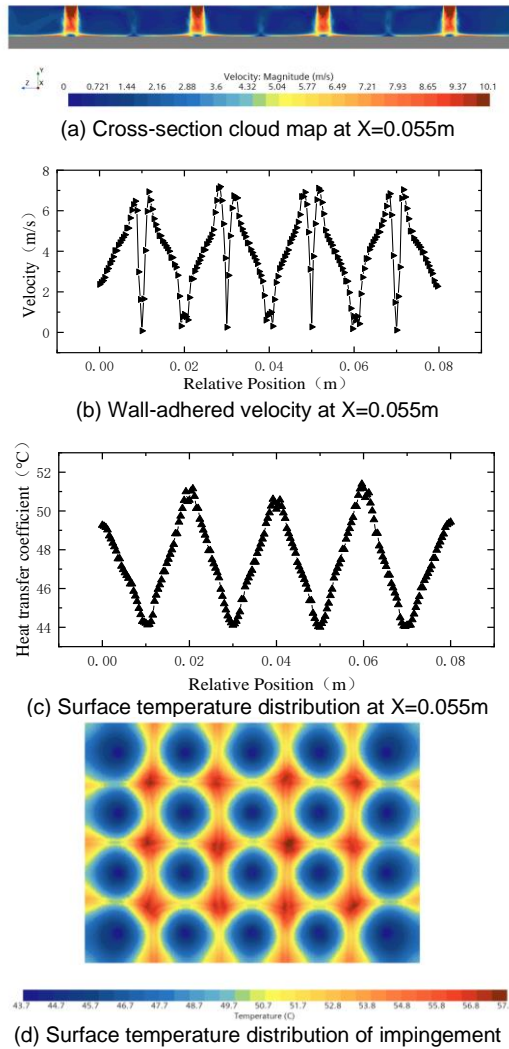


Fig. 5 Grid independence

## 3. Calculation Results and Analysis

### 3.1. Analysis of Heat Transfer Performance of Inline Array Jet Impingement Cooling.

The row-to-row distance ( $L_1$ ) of the inline jet holes is set to 22 mm, and the column-to-column distance ( $L_2$ ) is set to 20 mm.



**Fig. 6.** Analysis of Inline Jet Impingement Results at  $X=0.055\text{m}$

From Fig.6, it can be observed that the injected fluid enters the impingement heat transfer chamber through the orifice plate, and its velocity gradually decreases along the impingement direction. When the injected fluid impinges on the bottom plate, the velocity at the stagnation point is 0 m/s. At this point, the vertical velocity gradually converts to horizontal velocity and flows in the direction from the stagnation zone to the wall jet zone. The velocity of the injected fluid shows a trend of first increasing and then decreasing. When the injected fluid reaches the jet surge zone, the velocity shows a trend of first increasing and then decreasing. The temperature distribution on the surface which needs jet cooling follows the same pattern as the velocity distribution in the wall jet zone and jet surge zone. The stagnation point at the stagnation zone has the highest temperature, and as the velocity gradually converts from vertical velocity to horizontal velocity, the velocity increases and the heat transfer capability improves. As the injected fluid flows along the wall jet zone, its velocity gradually decreases, and the heat transfer performance decreases accordingly. In the jet surge zone, due to the interaction between different jets, the injected fluid adheres to the wall at the collision position, resulting in the highest wall-adhered velocity and the best heat transfer performance.

### 3.2. Influence of Inlet Temperature on Heat Transfer Surface.

The distance ( $H$ ) between the jet hole and the heat transfer surface is set to 5 mm, and the diameter ( $d$ ) of the jet hole is set to 2 mm. By changing the inlet temperature of the injected fluid, the influence of the inlet temperature on jet impingement cooling is studied. The inlet velocity is set to 6 m/s ( $Re=13483$ ), 8 m/s ( $Re=17977$ ), and 10 m/s ( $Re=22471$ ) for comparison. The range of inlet injected fluid temperature is  $10^\circ\text{C}$  to  $40^\circ\text{C}$ .

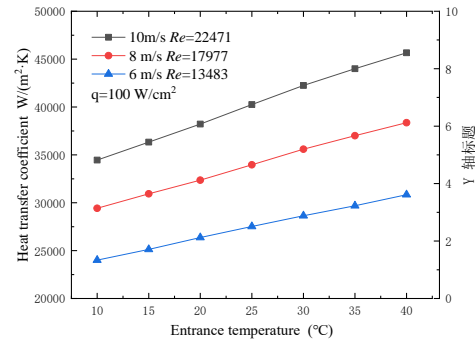


**Fig.7.** Influence of Inlet Temperature on Heat Transfer Surface

From Fig.7, it can be observed that as the inlet temperature increases, the heat transfer coefficient of the injected fluid impinging on the heat transfer surface gradually increases for different velocities. Through the analysis of the physical properties of the injected fluid, it is found that the inlet temperature mainly affects the thermal conductivity and viscosity of the injected fluid. The injected fluid absorbs heat from the heat transfer surface when it impinges on it, causing the temperature of the water to gradually rise. Higher inlet temperatures cause changes in the physical properties of the injected fluid, with the thermal conductivity being the most significant. The higher the temperature of the water, the higher its thermal conductivity, and the higher the heat transfer coefficient of the injected fluid impinging on the heat transfer surface. Properly increasing the inlet temperature promotes the enhancement of heat transfer capacity. The dynamic viscosity of the injected fluid mainly affects the flow resistance and the boundary layer thickness. When the dynamic viscosity decreases, the dynamic viscosity of the injected fluid decreases, and the thickness of the flow boundary layer becomes thinner. According to the boundary layer theory, when the boundary layer becomes thinner, the velocity gradient near the wall surface increases, and the heat transfer coefficient is proportional to the velocity gradient at the wall surface. Therefore, a decrease in dynamic viscosity also contributes to improving heat transfer capacity. The viscosity of water decreases with increasing temperature. From Fig.5, it can be observed that the higher the Reynolds number of the injected fluid, the greater the slope of the fitting curve of the inlet temperature and heat transfer coefficient. The increment of the injected fluid is beneficial to the discharge of the injected fluid and promotes the enhancement of the efficiency of the jet impact heat exchange. This study reveals that the heat transfer coefficient in jet impingement cooling significantly increases with higher heat flux density

and inlet temperature. While these results may be theoretically expected, the numerical simulations further confirm this relationship, providing substantial support for a deeper understanding of the heat transfer mechanisms in jet impingement cooling.

### 3.3. Influence of Height on Heat Transfer Performance.

The diameter ( $d$ ) of the jet hole is set to 2 mm, and Study the impact of height on jet impingement heat transfer by changing the Reynolds number. To study the effect of  $H/d$  on the heat transfer performance of jet impingement cooling, three different Reynolds numbers are selected. The heat flux density is set to  $100 \text{ W/cm}^2$ , and the inlet temperature ( $T_{in}$ ) is  $25^\circ\text{C}$ . The values of  $H/d$  studied in this paper are 1, 1.5, 2, 2.25, 2.5, 3, 4, and 5.

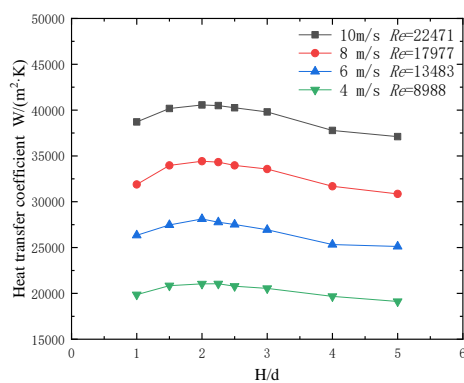


Fig.8. Influence of Height on Heat Transfer Performance

From Fig.8, it can be observed that as the ratio of height to diameter increases, the heat transfer coefficient of jet impingement cooling initially increases rapidly, reaches a peak, and then decreases gradually at a slower rate. By studying four different inlet velocities, it is found that the intervals of  $H/d$  where the heat transfer coefficient reaches its peak value differ for different inlet velocities within the range of  $H/d$  values studied in this paper. For an inlet velocity of  $4 \text{ m/s}$  ( $Re = 8988$ ), the heat transfer coefficient reaches its maximum value at  $H/d = 2.25$ , while for inlet velocities of  $6 \text{ m/s}$  ( $Re = 13483$ ),  $8 \text{ m/s}$  ( $Re = 17977$ ), and  $10 \text{ m/s}$  ( $Re = 22471$ ), the optimal heat transfer performance occurs at  $H/d = 2$ . Among different impingement velocities, the optimal height range for jet impingement heat transfer is not the same. Within the scope of this study, the optimal impingement height for inlet velocities of  $6 \text{ m/s}$  ( $Re = 13483$ ),  $8 \text{ m/s}$  ( $Re = 17977$ ), and  $10 \text{ m/s}$  ( $Re = 22471$ ) is between 1.5 and 2.25. The optimal height for inlet velocity of  $4 \text{ m/s}$  is between 2 and 2.5. The optimal impingement height for jet impingement heat transfer varies with different impingement velocities. In this study, As the Reynolds number increases, the optimal height of jet impingement cooling decreases accordingly. When the water impacts the heat transfer surface, vortex flow is formed due to the interaction between different jets. When the impingement height is relatively low, the upward vortex flow directly impacts the jet hole due to insufficient space, causing some of the injected fluid to re-enter the jet, thereby enhancing the heat transfer capacity of the jet. When the optimal height is reached,

the vortex flow re-enters the jet with the most injected fluid, resulting in the best heat transfer performance. After the jet is ejected from the nozzle, it undergoes entrainment, during which the energy of the jet continuously decreases. The higher the height, the more energy loss occurs in the impingement heat transfer. This weakens the heat transfer performance of jet impingement cooling.

### 3.4. Influence of Heat Flux Density on Heat Transfer Performance.

The distance ( $H$ ) between the jet hole and the heat transfer surface is set to 5 mm, and the diameter ( $d$ ) of the jet hole is set to 2 mm. By changing the velocity of the injected fluid, the influence of heat flux density on cold plate heat transfer is studied. The inlet velocity is set to  $6 \text{ m/s}$  ( $Re = 13483$ ),  $8 \text{ m/s}$  ( $Re = 17977$ ), and  $10 \text{ m/s}$  ( $Re = 22471$ ) for comparison. The injected fluid temperature is  $25^\circ\text{C}$ . The heat flux density is set to  $60\text{--}300 \text{ W/cm}^2$ . The surface temperature of the heat transfer surface under different flow rates is below  $100^\circ\text{C}$ , indicating single-phase heat transfer in jet impingement cooling. The heat transfer coefficient varies with the change in heat flux density and velocity, as shown in Fig.9.

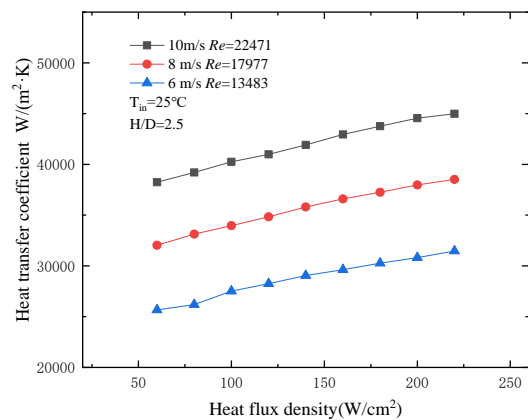


Fig. 9. Heat Transfer Coefficient on Heat Transfer Surface under Different Heat Flux Densities

Under a fixed flow rate, as the heat flux density increases, the surface heat transfer coefficient gradually increases. When the injected fluid flow rate increases to  $10 \text{ m/s}$  or decreases to  $6 \text{ m/s}$ , the change curve of the average heat transfer coefficient with heat flux density can be reshaped. It can be observed that the overall trend of the average heat transfer coefficient remains basically unchanged with the increment in heat flux density, but the absolute value of the average heat transfer coefficient increases with the increment in Reynolds number and decreases with the decrease in Reynolds number

### 3.5. Influence of Different Structures on Jet Impingement.

To reduce the local hot spot temperature and improve the overall temperature uniformity, the influence of different nozzle arrangement patterns on jet impingement heat transfer performance is studied. The nozzle arrangement is shown in Fig.10. The diameter ( $d$ ) of the nozzle is 2 mm, and  $H/d = 2$ . The inlet velocity is  $10 \text{ m/s}$  ( $Re = 22471$ ). The influence of the

arrangement on jet impingement cooling is studied by changing the inlet temperature of the injected fluid.

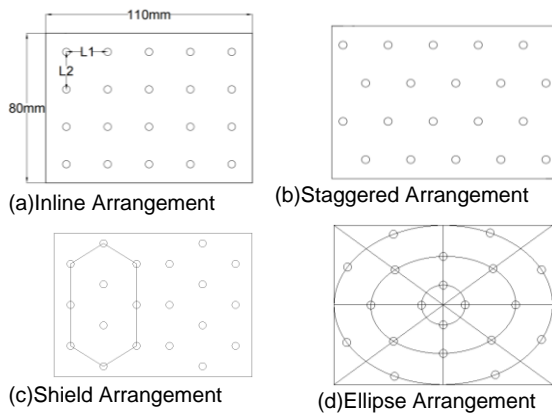


**Fig. 10.** Schematic Diagram of Different Nozzle Arrangement Patterns

The temperature distribution on the heat transfer surface under different nozzle arrangements is shown in Fig.11. Under high heat flux, there are localized hot spots in the jet impingement region for different nozzle arrangements. However, shield and elliptical arrangements help to achieve a more uniform temperature distribution within the heat transfer surface and concentrate the hot spots. In the study conducted in this paper, the nozzle arrangement did not improve the overall heat transfer performance.

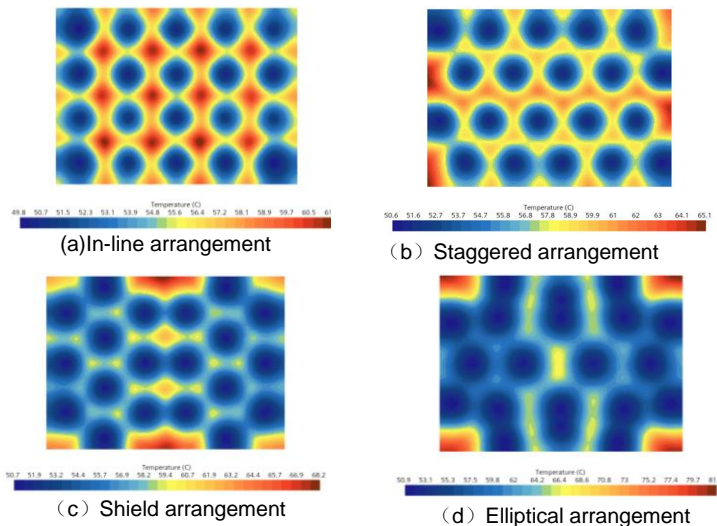


**Fig. 11.** shows the temperature contour of the conformal surface under different arrangements with  $T_{in}=25^{\circ}\text{C}$ .

To further investigate the impact of different structures on the jet impingement heat transfer performance, a flow deflector structure was added based on the in-line nozzle arrangement, with the flow deflector located at the projected position between adjacent nozzles on the base plate (as shown in Fig.12). The depth (a) and width (b) of the flow deflector were set as 1.5mm.

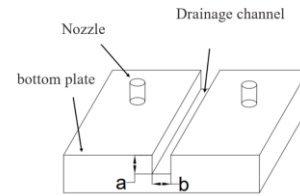


**Fig. 12.** Drainage channel Structure Diagram

The flow deflector structure on the base plate effectively improves the heat transfer performance of jet impingement and reduces the temperature of localized hot spots. Compared to the temperature of localized hot spots in the in-line arrangement, the temperature of localized hot spots in the flow deflector structure can be reduced by  $1.2^{\circ}\text{C}$ .

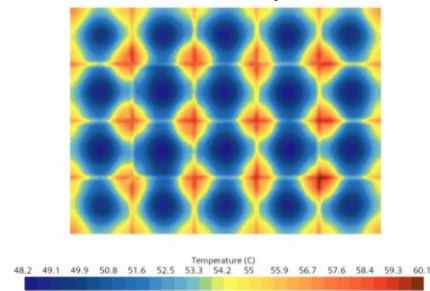


**Fig. 13.** Under the structure of the diversion groove, the temperature cloud map of the conformal surface.

To study the influence of different nozzle arrangements and flow deflector structures on the overall uniformity of the surface which needs jet cooling, calculations were performed by taking points on the surface which needs jet cooling (total  $220 \times 160$  points) using formulas (9), (10), and (11). The computational results are shown in Table 2. From the table, it can be seen that the temperature uniformity of the base plate with the flow deflector structure is higher than that of different nozzle arrangements. Among the nozzle arrangements, the ranking of non-uniformity is in-line < staggered < shield arrangement < elliptical arrangement.

**TABLE 2.** presents the overall non-uniformity of the surface which needs jet cooling under different nozzle structures.

Structure	Non-uniformity
In-line	5.71%
Elliptical arrangement	11.59%
Drainage channel	4.26%
Shield arrangement	6.86%
Staggered	6.11%

From Fig.14, it can be observed that the arrangement of nozzles affects the heat transfer performance of the heat transfer surface. Among them, the in-line arrangement exhibits the best heat transfer performance, with a maximum heat transfer coefficient of  $45663\text{W}/(\text{m}^2 \cdot \text{K})$ . The elliptical arrangement has the worst heat transfer performance, with a value of  $38468\text{W}/(\text{m}^2 \cdot \text{K})$ . The heat transfer performance of the staggered arrangement is better than that of the shield arrangement. The in-line arrangement shows the highest

improvement in heat transfer performance compared to the elliptical arrangement, with a maximum enhancement of 7.29%. Under the same conditions, the maximum heat transfer coefficient of the surface which needs jet cooling with the flow deflector structure reaches  $48650\text{W}/(\text{m}^2\cdot\text{K})$ , which increases the maximum heat transfer performance by 6.53% compared to the optimal structure of nozzle arrangement. By comparing different structures, it is found that under the same conditions, the base plate with the flow deflector structure can enhance the overall heat transfer capacity of jet impingement and effectively reduce the temperature of localized hot spots.

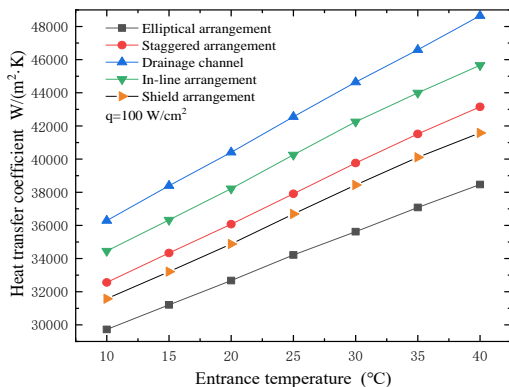


Fig. 14 illustrates the influence of nozzle arrangement on heat transfer performance.

## Conclusion

In this paper, numerical simulations were conducted to study the characteristics of array jet impingement heat transfer, focusing on the effects of heat flux density, inlet temperature, jet height, array arrangement, and flow deflector structure on jet impingement cooling performance and temperature distribution uniformity. The specific research conclusions are as follows:

1. The heat transfer coefficient of jet impingement cooling increases with the increment of heat flux density and inlet temperature, with the main influence on injected fluid temperature. The thermal conductivity increases with the increment of injected fluid temperature, which is beneficial for promoting jet impingement heat transfer. In addition, the temperature increase leads to a decrease in viscosity, resulting in a thinner boundary layer and improved heat transfer performance.
2. Jet impingement cooling has an optimal height. In the content studied in this paper, the optimal height range for jet impingement cooling is between  $H/d=1.5$  and 5. The higher the velocity, the lower the optimal height range. For jet impingement with inlet velocities of 6 m/s, 8 m/s, and 10 m/s, the optimal impingement height ranges between 1.5 and 2.25. The best impingement height for an inlet velocity of 4 m/s is between 2 and 2.5.
3. Under a heat flux density of  $100\text{ W}/\text{cm}^2$ , nozzle arrangement does not improve the heat transfer performance. The temperature uniformity of in-line arrangement > staggered > shield arrangement > elliptical arrangement. The

temperature uniformity of the in-line nozzle arrangement is 88% higher than that of the elliptical arrangement, and the heat transfer performance is improved by 7.29%.

4. The flow deflector structure performs better in heat transfer capacity than nozzle arrangement. The flow deflector structure increases the heat transfer capacity by 53% compared to the in-line nozzle arrangement. The temperature uniformity is also increased, with a 1.45% improvement compared to the in-line arrangement.

## References :

- [1] R Viswanath, V Wakharkar, A Watwe, and V Lebonheur, 'Thermal Performance Challenges from Silicon to Systems', p. 16, 2000.
- [2] M. A. Ebadian and C. X. Lin, "A Review of High-Heat-Flux Heat Removal Technologies," *Journal of Heat Transfer*, vol. 133, no. 11, p. 110801, Nov. 2011, doi: 10.1115/1.4004340.
- [3] S.M. Sohel Murshed, C.A. Nieto de Castro, "A critical review of traditional and emerging techniques and fluids for electronics cooling," *Renewable and Sustainable Energy Reviews*, vol. 78, pp. 821–833, Oct. 2017, doi: 10.1016/j.rser.2017.04.112.
- [4] D Dan, "The Latest research progress and evaluation of Computer chip cooling technology," *Modern Computer (Professional Edition)*, no. 23, pp. 26–30, 2014. DOI:10.3969/j.issn.1007-1423.2014.08.006.
- [5] M. Molana and S. Banooni, "Investigation of heat transfer processes involved liquid impingement jets: a review," *Braz. J. Chem. Eng.*, vol. 30, no. 3, pp. 413–435, Sep. 2013, doi: 10.1590/S0104-66322013000300001.
- [6] A. Ianiro and G. Cardone, "Heat transfer rate and uniformity in multichannel swirling impinging jets," *Applied Thermal Engineering*, vol. 49, pp. 89–98, Dec. 2012, doi: 10.1016/j.applthermaleng.2011.10.018.
- [7] M. J. Rau and S. V. Garimella, "Local two-phase heat transfer from arrays of confined and submerged impinging jets," *International Journal of Heat and Mass Transfer*, vol. 67, pp. 487–498, Dec. 2013, doi: 10.1016/j.ijheatmasstransfer.2013.08.041.
- [8] A. J. Robinson and E. Schnitzler, "An experimental investigation of free and submerged miniature liquid jet array impingement heat transfer," *Experimental Thermal and Fluid Science*, vol. 32, no. 1, pp. 1–13, Oct. 2007, doi: 10.1016/j.exptthermflusci.2006.12.006.
- [9] P. Tie, Q. Li, and Y. Xuan, "Investigation on the submerged liquid jet arrays impingement cooling," *Applied Thermal Engineering*, vol. 31, no. 14–15, pp. 2757–2763, Oct. 2011, doi: 10.1016/j.applthermaleng.2011.04.048.
- [10] M. Imbriale, A. Ianiro, C. Meola, and G. Cardone, "Convective heat transfer by a row of jets impinging on a concave surface," *International Journal of Thermal Sciences*, vol. 75, pp. 153–163, Jan. 2014, doi: 10.1016/j.ijthermalsci.2013.07.017.
- [11] C. S. Kumar and A. Pattamatta, "Assessment of Heat Transfer Enhancement Using Metallic Porous Foam Configurations in Laminar Slot Jet Impingement: An Experimental Study," *Journal of Heat Transfer*, vol. 140, no. 2, p. 022202, Feb. 2018, doi: 10.1115/1.4037540.
- [12] A. M. Kuraan, S. I. Moldovan, and K. Choo, "Heat transfer and hydrodynamics of free water jet impingement at low nozzle-to-plate spacings," *International Journal of Heat and Mass Transfer*, vol. 108, pp. 2211–2216, May 2017, doi: 10.1016/j.ijheatmasstransfer.2017.01.084.
- [13] R. Jenkins, R. Lupoi, R. Kempers, and A. J. Robinson, "Heat transfer performance of boiling jet array impingement on micro-grooved surfaces," *Experimental Thermal and Fluid Science*, vol. 80, pp. 293–304, Jan. 2017, doi: 10.1016/j.exptthermflusci.2016.08.006.
- [14] J.Z. Zhang, Y.K.Li, X.M Tan, and L.Li, "Numerical calculation and experimental study of local convective heat transfer characteristics of jet array impact cooling," *Acta Aeronautica et Astronautica Sinica*, no. 4, pp. 339–342, 2004. DOI:10.3321/j.issn:1000-6893.2004.04.004.
- [15] Y. Xing, S. Spring, and B. Weigand, "Experimental and Numerical Investigation of Heat Transfer Characteristics of In-line and Staggered Arrays of Impinging Jets," *Journal of Heat Transfer*, vol. 132, no. 9, p. 092201, Sep. 2010, doi: 10.1115/1.4001633.
- [16] D. H. Rhee, J. H. Choi, and H. H. Cho, "Heat (Mass) Transfer on Effusion Plate in Impingement/Effusion Cooling Systems," *Journal of*

- Thermophysics and Heat Transfer*, vol. 17, no. 1, pp. 95–102, Jan. 2003, doi: 10.2514/2.6739.
- [17] F.b. Zhang, Y.C.Zhang, and L.J Yang, "Influence of circular nozzle internal structure on jet impact heat transfer performance," *Journal of Northeastern University (Natural Science Edition)*, vol. 39, no. 9, pp. 1257-1261, 2018.
- [18] Z. Li R.F Dou and Z.Zhi, "Numerical simulation of single-hole jet impact flow and heat transfer process," *Industrial Furnace*, vol. 33, no. 4, pp. 1-7, 2011. DOI:10.3969/j.issn.1001-6988.2011.04.001.
- [19] X.He, " Experimental research and numerical simulation of laminar flow cooling of matrix arrangement nozzles " M.A. thesis,anhui university, 2021. DOI: 10.27790/d.cnki.gahgy.2020.000181.
- [20] Y. Liu, Y. Rao, and L. Yang, "Numerical simulations of a double-wall cooling with internal jet impingement and external hexagonal arrangement of film cooling holes," *International Journal of Thermal Sciences*, vol. 153, p. 106337, Jul. 2020, doi: 10.1016/j.ijthermalsci.2020.106337.
- [21] M .Yu, Z .Wang, D .Li,and W.Wang,"Experimental Performance Study of jet impact cooling system," *Cryogenic Engineering*, no. 6, pp. 50-55+69, 2010. DOI:10.3969/j.issn.1000-6516.2010.06.012.
- [22] D. LI, "Simulation and Experimental Study of Jet Cooling Device," M.A. thesis, Shanghai Jiao Tong University, 2010.